

Proceedings of the Korean Nuclear Society Spring Meeting
Cheju, Korea, May 2001

Corrosion Characteristics of PT-7M and PT-3V Titanium Alloys in Ammonia Water Chemistry

Byoung-Kwon Choi, Tae-Kyu Kim, Yong-Hwan Jeong, Doo-Jeong Lee, Moon-Hee Chang

Korea Atomic Energy Research Institute
P.O.Box 105, Yusung, Taejon 305-600, Korea

ABSTRACT

The corrosion characteristics of titanium alloys and the welded joints in these alloys have been evaluated at 360 °C in the ammonia water chemistry of a pH 9.98 using a recirculating loop system. PT-7M titanium alloy showed a recrystallization structure (α alloy) containing an Al-rich precipitate ($\text{Al}_3(\text{Ti}, \text{Zr})_{0.75}\text{Fe}_{0.25}$). PT-3V titanium alloy revealed a fully lamellar structure ($\alpha+\beta$ alloy) containing Ti_3Al precipitates (α_2) in the α -layers. These titanium alloys showed a superior corrosion resistance, because of the formation of the anatase and rutile oxides. As the corrosion proceeds, the surface color of PT-7M varied from white light to deep blue within 30 days, further to light blue after 100 days. The welded titanium alloys showed the accelerated corrosion rates than their base metals, since the HAZ and filler metal in these alloys preferentially contributed to the corrosion. After the corrosion time of 100 days, the values of hydrogen contents in PT-7M and PT-3V titanium alloys appeared to be 53.3 and 33.2 ppm, respectively.

1. INTRODUCTION

Desalination technologies have been developed over the last 40 years in view of water production from sea or blackish water, and become a reliable industrial process in the regions of severe water shortage: Caribbean, North Africa, middle-east Asia and south-east region of USA. As one of various desalination processes, SMART (System-integrated Modular Advanced Reactor) has been recently developed for the electricity generation and sea water desalination.

SMART is a small-sized advanced integral PWR (Pressurized Water Reactor) that is designed to produce 330 MW of thermal energy under full power operating conditions. Major primary components are integrated within a single pressure vessel, in which the arrangement of components differs from that of the conventional loop-type reactors.

The reactor assembly of SMART contains major primary systems such as fuel and core, steam generator (SG), control element drive mechanism (CEDM) and so on. For the SMART materials, titanium alloys have been recently paid much attention as a candidate material for steam generator in SMART, because of their low density and high strength values, excellent corrosion resistance to many mineral acids and chlorides, low disposition to vacancy swelling, low disposition to be activated in neutron flux, and suitable durability characteristics [1-6].

With respect to the water chemistry in SMART, the ammonia water chemistry (pH 9.5-10.5 at 25 °C) is strongly considered as a primary coolant water chemistry. However, there is little identification about the stability of titanium alloys in contact with ammonia water chemistry at an elevated temperature. In addition, it is expected that the welded joint of titanium alloys, when they are exposed to an ammonia aqueous solution, would show a different corrosion behavior.

This study has been performed to evaluate the corrosion characteristics of PT-7M and PT-3V titanium alloys for steam generator in SMART and their welded joints of these alloys at 360 °C in the ammonia water chemistry of a pH 9.98. The corrosion behavior of titanium alloys has been principally evaluated using a recirculating loop system.

PT-7M: CAS Registry number 66082-54-0 (American Chemical Society).

PT-3V: CAS Registry number 37329-52-5 (American Chemical Society).

2. EXPERIMENTAL PROCEDURES

PT-7M tube (25 mm L. × 6 mm I.D. × 10 mm O.D. in size) and PT-3V rolled sheet (25 mm L. × 30 mm W. × 5 T. in size) were prepared for the corrosion test. Their chemical compositions are analyzed and given in Table 1. Their microstructures were examined using a Transmission Electron Microscope (TEM).

The out-pile corrosion tests were conducted at 360 °C for 100 days using a recirculating loop system under a pressure of 2,680 psi. An exposure environment of the alloys was the ammonia aqueous solution adjusted to a pH 9.8 at 25 °C using a dilute NH₄OH solution. The corrosion resistance of the alloys was continuously evaluated by measuring their weight gain per unit

surface area in relation to the exposure time. The oxide studies were performed using a scanning electron microscopy (SEM) and a X-ray diffraction (XRD). The content of hydrogen absorbed was also analyzed.

3. RESULTS AND DISCUSSION

3.1 Microstructures of PT-7M and PT-3V titanium alloys

Fig. 1 shows a bright field TEM image in the longitudinal section of PT-7M titanium alloy. This alloy showed a fully recrystallization structure of hcp α titanium alloy with an average grain size of about 20 μ m. No bcc β phase is observed. This observation means that the final annealing after the final pilgering stage in the manufacturing route of this alloy would be below $\alpha \rightarrow \beta$ transition temperature.

Fig. 2 shows TEM/EDS results of the matrix and precipitation in PT-7M titanium alloy. An examination of the precipitates in this alloy revealed that most of precipitates were an Al-rich precipitation with an average size of 100 nm. The chemical composition of the precipitate was determined to be (wt.%) 72.34Ti, 3.12Al, 24.36Zr, and 0.27Fe, whereas that of the matrix was analyzed to be (wt.%) 94.53Ti, 2.16Al, 3.24Zr, and 0.07Fe. The crystal structure of precipitate was identified as a face-centered cubic (fcc, $a = 0.3942$ nm) with a chemical formulation of $\text{Al}_3\text{Ti}_{0.75}\text{Fe}_{0.25}$. The Zr can be substituted with Ti, because they have same crystal structures of a hcp. Thus, the chemical formulation of precipitation would be again written as $\text{Al}_3(\text{Ti}, \text{Zr})_{0.75}\text{Fe}_{0.25}$.

Fig. 3 shows a bright field TEM image of PT-3V titanium alloy. This alloy revealed a lamellar structure of $\alpha + \beta$ titanium alloy. The width size of the individual α -lamellae is about 2 μ m. The microstructure of $\alpha + \beta$ alloy like PT-3V titanium alloy is usually determined by the cooling rate from the β phase, since the recrystallization kinetics in the β phase field are so fast. That is, the size of the α -colonies as well as the size of the individual α -lamellae are reduced with increasing cooling rate from the β grains.

Fig. 4 shows TEM/EDS results of the matrix and precipitation in PT-3V titanium alloy. TEM micrograph of PT-3V titanium alloy showed the precipitates with a size of 100 nm in the α phase matrix. The chemical composition of the precipitate was determined to be (wt.%) 92.90Ti, 4.77Al, 2.18V, and 0.15Fe, whereas that of the matrix was analyzed to be (wt.%) 93.24Ti, 4.00Al, 2.74V, and 0.11Fe. The precipitate in PT-3V was identified as α_2 precipitate (hexagonal, $a = 0.577$ nm, $c = 0.462$ nm) with a chemical formulation of Ti_3Al . For nearly all $\alpha+\beta$ Ti-alloys, the α phase is age-hardened by the precipitation of very small, coherent Ti_3Al particles (α_2)

during the final low temperature heat-treatment. It is known that the volume fraction of these α_2 precipitates depends on the oxygen content of $\alpha+\beta$ titanium alloy, because oxygen is known to stabilize the α_2 phase [7].

Fig. 5 shows SEM micrographs of the welded joint of PT-3V titanium alloy. The welded joint of PT-3V showed three distinct microstructures: matrix, bond of weld and heat affected zone (HAZ). It is observed that the size of the individual α -lamellae in the HAZ has much narrower than that in the matrix. A large number of precipitates with a size of about 5 μm and voids are observed in the HAZ; the precipitates are also considered as Ti_3Al particles (α_2). As mentioned before, the microstructure of PT-3V titanium alloy ($\alpha+\beta$ Ti-alloy) is mainly controlled by the cooling rate. It is thus considered that the cooling rate in the HAZ had a considerably fast, giving the narrow size of the individual α -lamellae.

3.2 Corrosion behavior

Fig. 6 shows the corrosion behavior of PT-7M and PT-3V titanium alloys at 360 °C in the ammonia aqueous solution of a pH 9.98. The PT-7M and PT-3V titanium alloys showed an excellent corrosion resistance, since their weight gains after the exposure time of 100 days appeared to be about 2.4 and 1.7 mg/dm^2 , respectively. The superior corrosion resistance of titanium is usually provided by a tenacious oxide layer as a result of an affinity of titanium for oxygen. The oxide layer is stable and hard, thereby increasing the resistance to corrosion. For the corrosion resistance of two titanium alloys, it is observed that PT-3V has a slightly superior corrosion resistance than PT-7M until the exposure time of 100 days.

Fig. 7 shows the variation of surface appearance of PT-7M and PT-3V titanium alloys with corrosion time at 360 °C in the ammonia aqueous solution of a pH 9.98. As the corrosion proceeds, the variation of surface appearance of titanium alloys is observed. In PT-7M, the surface color varied from white light to deep blue after 30 days. As the corrosion proceeds, the deep blue color varied to light blue, and further to brown after 100 days. Meanwhile, the surface color of PT-3V varied to dark brown after 15 days. After 30 days, blue color is observed on the base of brown surface. It is considered that the variation of surface color of titanium alloy is due to the formation of oxides, growth of oxide layers, and transformation of oxide structure.

Fig. 8 shows the effect of welding on the corrosion behavior of PT-3V titanium alloy at 360 °C in the ammonia aqueous solution of a pH 9.98. It is observed that the welded PT-3V titanium alloy showed an accelerated corrosion rate than PT-3V matrix. This means that the welding has an influence on the corrosion resistance of titanium alloy, and accelerates the corrosion rate. It is possible to explain in terms of the change in the microstructure of PT-3V titanium alloy by the

welding as shown in Fig. 5. It is believed that the narrow size of the individual α -lamellae, the enlarged precipitates and a large amount of voids formed by the welding would be main reason to accelerate the corrosion rate.

Fig. 9 shows the variation of surface appearance of the welded joints of PT-7M and PT-3V titanium alloys with corrosion time at 360 °C in the ammonia aqueous solution of a pH 9.98. Most of the welded materials have three distinct zones: filler metal, HAZ and matrix. It is observed that three distinct zones show a different corrosion rate each other, because they reveal a difference color on their surfaces at intervals of corrosion time. As the corrosion proceeds, the color of the HAZ and filler metal zone preferentially varied to dark blue. The corrosion of titanium alloy induces the variation of surface color as shown in Fig. 7. This observation indicates that the HAZ and filler metal zone would be a main source to promote the corrosion rate of the welded PT-3V titanium alloy examined in the present study.

Fig. 10 shows SEM micrographs of oxide surfaces at the metal-oxide interface of the matrix and HAZ of PT-7M titanium alloy corroded at 360 °C in the ammonia aqueous solution of a pH 9.98 for 100 days. The morphology of oxide surface at the metal-oxide interface in the matrix of PT-7M appeared to be a finely uniform oxide layer whilst that in the HAZ of this alloy revealed a rough one. This means that the HAZ promotes the rough oxide layer, accelerating the corrosion rate as shown in Fig. 9.

Fig. 11 shows X-ray diffraction patterns of PT-7M titanium alloy corroded for 7, 30 and 100 days at 360 °C in the ammonia aqueous solution of a pH 9.98. The most of oxides formed in this alloy until the corrosion time of 30 days are identified as an anatase (tetragonal, $a = 0.3786$ nm, $c = 0.9517$ nm, $c/a = 2.5$). In the oxides formed in PT-7M corroded for 100 days, two kinds of oxides, anatase and rutile (tetragonal, $a = 0.4594$ nm, $c = 0.2959$ nm, $c/a = 0.6$), are observed. The anatase is usually formed in the pressure below a pressure of 195,750 psi (13.5 kbar) at 360 °C [8]. The rutile is a product transformed from the anatase phase, because the anatase is a metastable phase in TiO_2 oxides. It is possible to consider from these results that the anatase oxide is mainly formed on the surface of titanium alloy at an early stage of corrosion, and the anatase transforms to rutile oxide as the thickness of oxide increase. When rutile phase is formed, the corrosion rate is going to reduce (Fig. 6). It is considered that the rutile phase would be more effective to disturb the diffusion of oxygen throughout oxide layer, because the c/a ratio of rutile is much smaller than that of the anatase. It resulted in the reduction of corrosion rate after an exposure time of 30 days, when the rutile phase is formed as a result of transformation from a metastable anatase phase. It is also possible to consider that the anatase formed on the surface of PT-7M titanium alloy shows deep bluish color, and the transformation

of anatase to rutile leads to the color variation from deep blue to light one as shown in Fig. 7.

3.3 Hydrogen pickup

Fig. 12 shows the hydrogen contents and hydrogen pickup fraction of PT-7M and PT-3V titanium alloys corroded at 360 °C in the ammonia aqueous solution of a pH 9.98 for 100 days. Titanium alloys have been paid much attention to the hydrogen pickup, because of the hydrogen embrittlement [9-16]. The PT-7M and PT-3V titanium alloys corroded for 100 days showed the hydrogen contents of 53.3 and 33.2 ppm, respectively (note that the initial hydrogen contents of PT-7M and PT-3V titanium alloys were 47 and 30 ppm, respectively). The values of hydrogen pickup fractions of these alloys were calculated as 0.94 and 0.69%, respectively. Room temperature solubility of hydrogen in titanium alloys is typically cited as ranging from 20 to 200 ppm. It is interesting to notice that the value of hydrogen pickup fraction in PT-3V is much lower than that in PT-7M. However, the solubility of hydrogen in titanium alloys is lower in alloys containing oxygen [17]. It is thus considered that the formation of hydride in PT-3V would be more easier than in PT-7M, because PT-3V titanium alloy contains greater oxygen content than PT-7M one (note that the initial oxygen contents of PT-7M and PT-3V titanium alloys before corrosion were 40 and 825 ppm, respectively).

4. CONCLUSIONS

The corrosion characteristics of PT-7M and PT-3V titanium alloys considered as materials for steam generator tube in SMART have been evaluated at 360 °C in the ammonia water chemistry of a pH 9.98 using a recirculating loop system. The following conclusions are drawn;

1. PT-7M titanium alloy showed a fully recrystallization structure (α alloy) with precipitates ($\text{Al}_3(\text{Ti}, \text{Zr})_{0.75}\text{Fe}_{0.25}$) whilst PT-3V titanium alloy revealed a lamellar structure ($\alpha + \beta$ alloy) with α_2 precipitates (Ti_3Al).
2. The PT-7M and PT-3V titanium alloy showed an excellent corrosion resistance, because a tenacious oxide layer identified as anatase and rutile phases formed on the surfaces of these alloys.
3. The welded titanium alloys showed an accelerated to the corrosion rate than the base materials, as the HAZ and filler metal in the welded joints of these alloys preferentially attributed to the corrosion.
4. The oxide transformation of metastable anatase to stable rutile phase tended to reduce the

corrosion rate, because the tetragonal rutile phase with the c/a ratio of 0.6 would be more effective to disturb the diffusion of oxygen throughout oxide layer than the tetragonal anatase phase with the c/a ratio of 2.5.

5. The PT-3V titanium alloy corroded for 100 days showed the lower hydrogen content than PT-7M titanium alloy (53.3 ppm in PT-7M and 33.2 ppm in PT-3V). However, the solubility of hydrogen in PT-3V containing oxygen content of 825 ppm would be much lower than in PT-3V containing the oxygen content of 40 ppm.

ACKNOWLEDGEMENTS

This work has been supported by the Korean Ministry of Science and Technology.

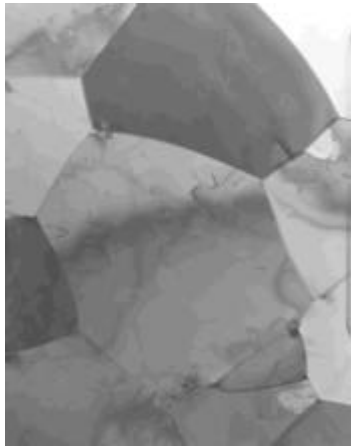
REFERENCES

1. O.A. Kozhevnikov, E.V. Nesterova, V.V. Rybin and I.I. Yarmolovich: *J. Nuclear Mater.* 271&272 (1999) 472-477
2. Gorynin, I.V.: *Materials Science and Engineering*, A263 (1999) 112-116
3. J.C. Williams: *M Materials Science and Engineering*, A263 (1999) 107-111
4. D.G. Kolman and J.R. Scully: *J. Electrochem. Soc.* 143 (1996) 1847-1860
5. E. Rolinski, G. Sharp, D.F. Cowgill and D.J. Peterman: *J. Nuclear Mat.* 252 (1998) 200-208
6. S.V. Gnedenkov, P.S. Gordienko, S.L. Sinebrukhov, O.A. Khrisanphova, and T.M. Skorobogatova: *Corrosion*, 56 (2000) 24-31
7. M.L. Wasz, F.R. Brotzen, R.B. Mclellan, and A.J. Griffin, Jr: *International Materials Reviews* 41 (1) (1996) pp. 1-12
8. J.L. Murray and H.A. Wriedt: *Bull. Alloy phase diagrams*, 1987, 8, 148-165
9. E. Fromm: *Z. physik. Chem. NF.* 147 (1986) 61-75
10. K. Nakasa and H. Satoh, *Corrosion Sci.*, 38 (1996) 457.
11. H.D. Kessler, R.G. Sherman and J.F. Sullivan: *J. Met.*, 7 (1955) 242-246
12. G.A. Lenning, J.W. Sprietnak, and R.I. Jaffee: *Trans. AIME*, 206 (1956) 1235-1240
13. D.A. Meyn, *Metall. Trans.*, 5 (1974) 2405.
14. J.C.M. Li, R.A. Oriani and L.S. Darken, *Z. Phy. Chem.*, 49 (1966) 271.
15. W.J. Pardee and N.E. Paton, *Metall. Trans.*, 11A (1980) 1301.
16. A.W. Sommer and D. Eylon, *Metall. Trans.*, 14A (1983) 2178.
17. G. Lutjering: *Materials Science and Engineering A263* (1999) 117-126

Table 1. Chemical compositions of PT-7M and PT-3V titanium alloys analyzed.

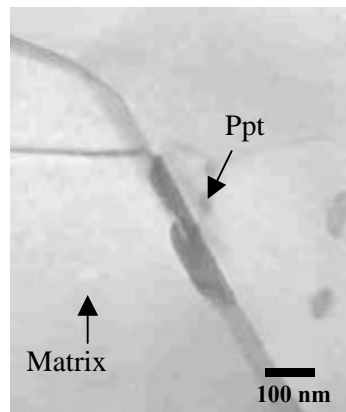
Alloy	Ti	Al	Zr	V	Fe	Co	C	H*	O*	N*
PT-7M	95.17	2.19	2.35	0.05	0.06	0.15	0.016	47	40	6
PT-3V	93.56	4.51	-	1.63	0.06	-	0.051	30	825	59

* is ppm, others are wt. %

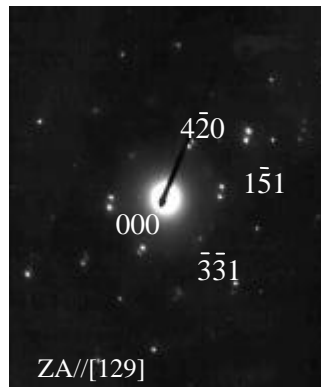


4 μm

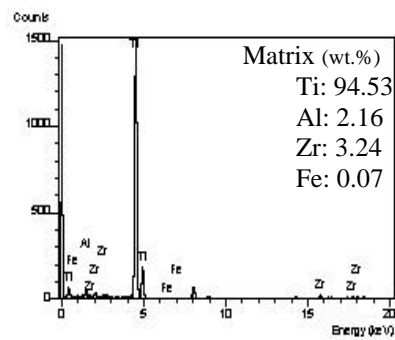
Fig. 1. Bright field TEM image of PT-7M titanium alloys showing a recrystallization structure with an average grain size 20 μm.



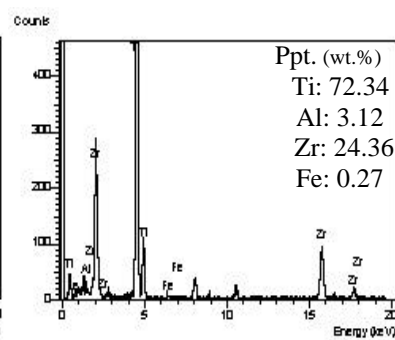
(a)



(b)



(c)



(d)

Fig. 2. TEM/EDS results of matrix and precipitation in PT-7M titanium alloy: (a) bright-field image, (b) selected area diffraction pattern from precipitation allowed in (a), (c) spectrum from matrix, and (d) spectrum from precipitation.



Fig. 3. Bright field TEM image of PT-3V titanium alloy ($\alpha+\beta$ Ti-alloy) showing a lamellar structure.

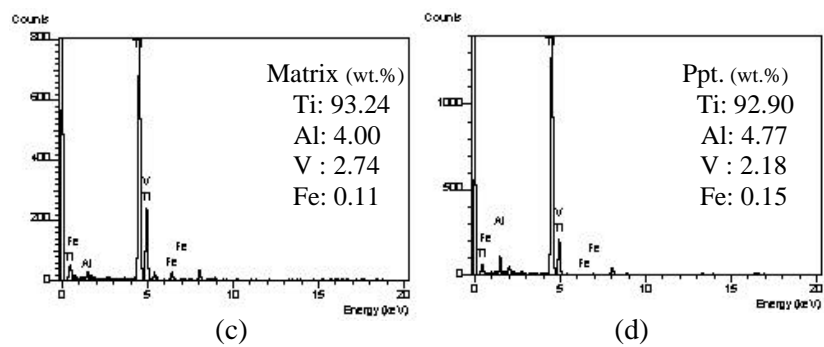
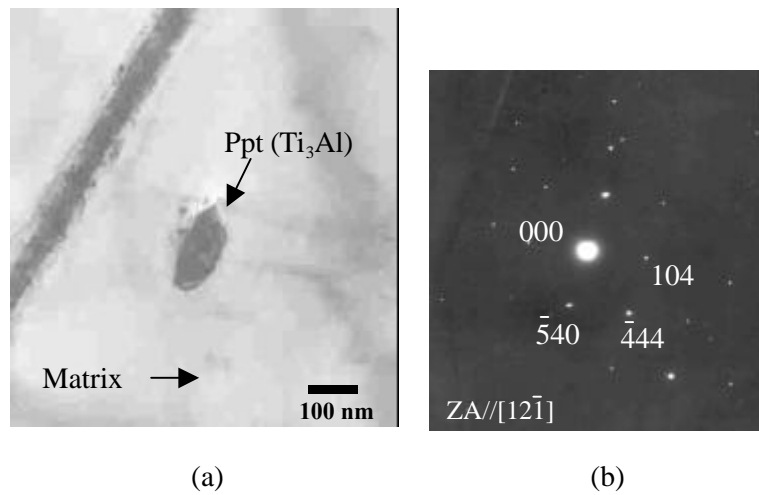
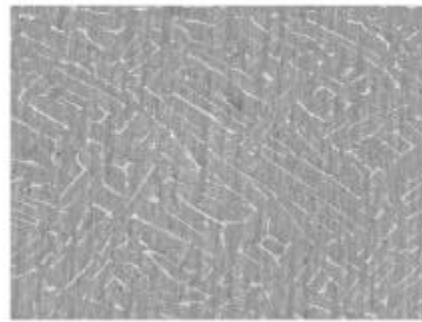
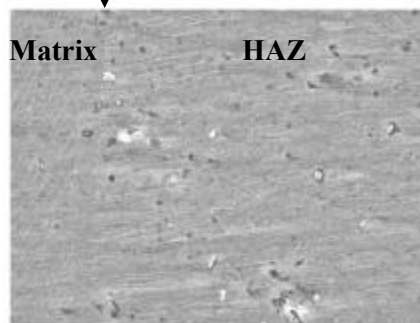


Fig. 4. TEM/EDS results of matrix and precipitation in PT-3V titanium alloy: (a) bright-field image, (b) selected area diffraction pattern from precipitation allowed in (a), (c) spectrum from matrix, and (d) spectrum from precipitation.

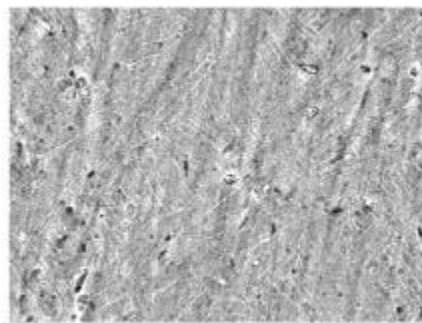


(a)

Bond of Weld



(b)



(c)

Fig. 5. SEM micrographs of weld joint of PT-3V titanium alloy: (a) matrix, (b) bond of weld, and (c) heat affected zone (HAZ)

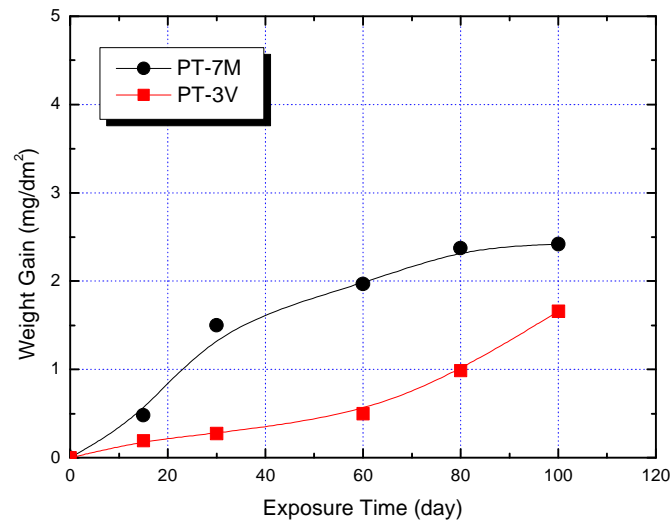


Fig. 6. Corrosion behavior of PT-7M and PT-3V titanium alloys at 360 in the ammonia aqueous solution of a pH 9.98.

	As-received	Corrosion time (day)			
		15	30	60	100
PT-7M					
PT-3V					

Fig. 7. Variation of surface appearance of PT-7M and PT-3V titanium alloys with corrosion time at 360 in the ammonia aqueous solution of a pH 9.98.

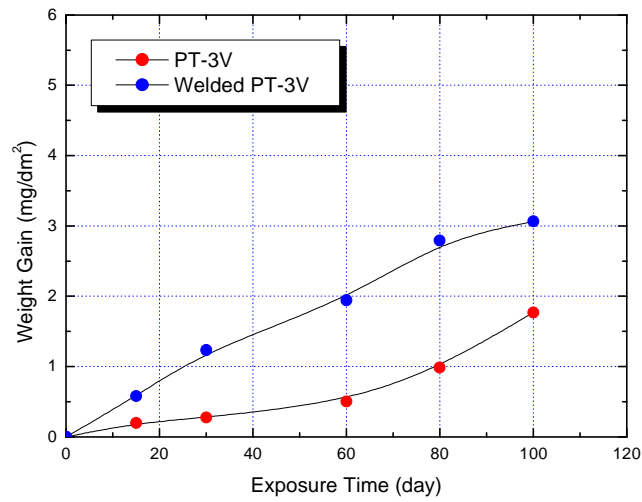


Fig. 8. Effect of welding on the corrosion behavior of PT-3V titanium alloy at 360 in the ammonia aqueous solution of a pH 9.98.

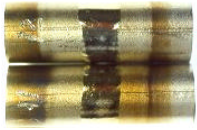

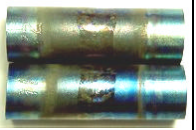

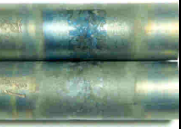


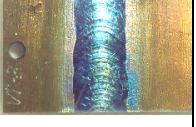


	As-received	Corrosion time (day)			
		15	30	60	100
Welded PT-7M					
Welded PT-3V					

Fig. 9. Variation of surface appearance of the welded joints of PT-7M and PT-3V titanium alloys with corrosion time at 360 in the ammonia aqueous solution of a pH 9.98.

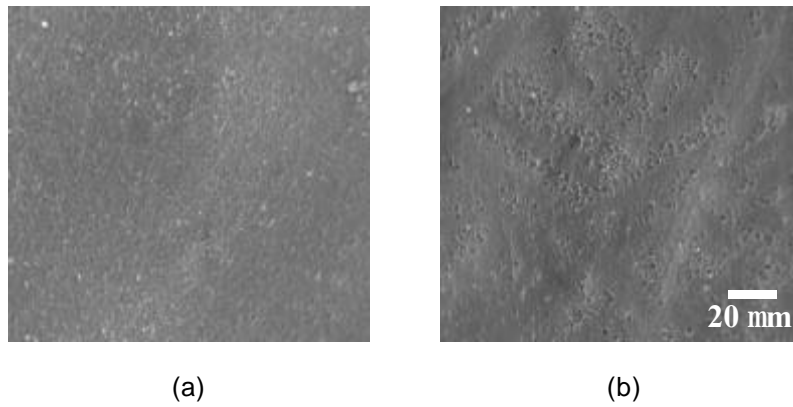


Fig. 10. SEM micrographs of oxide surfaces at the metal-oxide interface of PT-7M titanium alloy corroded at 360 °C in an ammonia aqueous solution of a pH 9.98 for 100 days: (a) matrix and (b) heat affected zone.

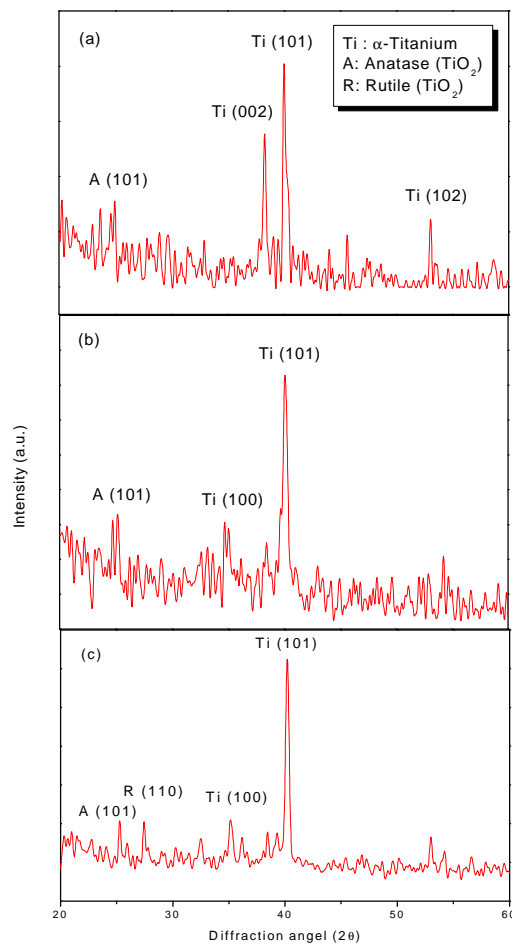


Fig. 11. X-ray diffraction patterns of PT-7M titanium alloy corroded at 360 °C in the ammonia water chemistry for (a) 7, (b) 30, and (c) 100 days.

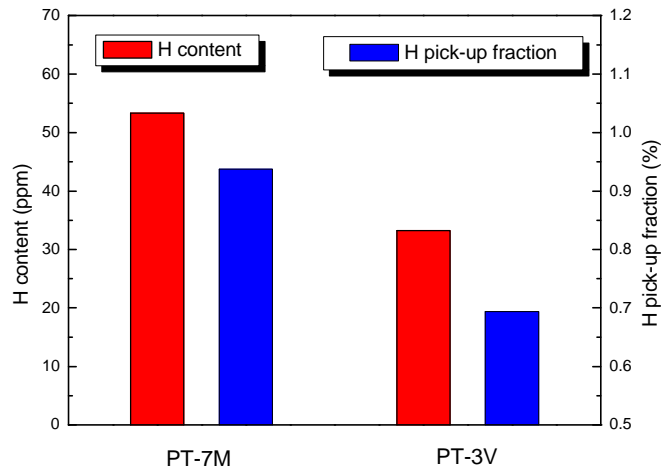


Fig. 12. Hydrogen contents and hydrogen pick-up fraction of PT-7M and PT-3V titanium alloys corroded at 360 °C in the ammonia aqueous solution of a pH 9.98 for 100 days